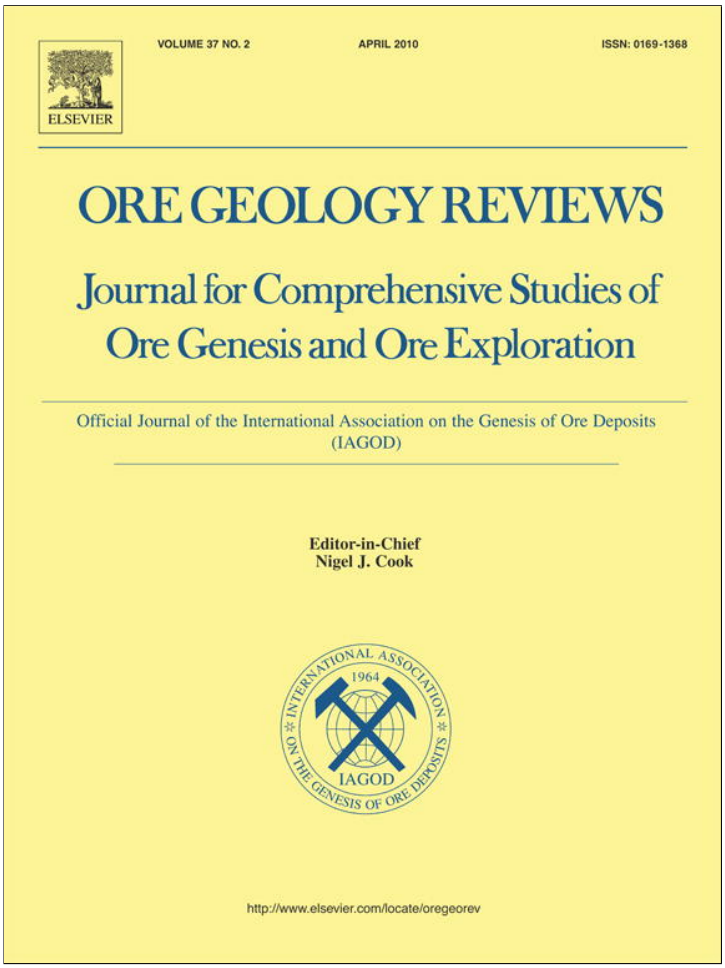

Ore Geology Reviews 37 (2010) 114–126

Contents lists available at ScienceDirect

Ore Geology Reviews

journal homepage: www.elsevier.com/locate/oregeorev

Geological and geochemical characteristics and ore genesis of the Keketale VMS Pb–Zn deposit, Southern Altai Metallogenic Belt, NW China

Bo Wan [a,b,*], Lianchang Zhang [a], Wenjiao Xiao [b]

[a] Key Laboratory of Mineral Resources, Institute of Geology and Geophysics, Chinese Academy of Sciences, P.O. Box 9825, Beijing 100029, P.R. China
[b] State Key Laboratory of Lithospheric Evolution, Institute of Geology and Geophysics, Chinese Academy of Sciences, P.O. Box 9825, Beijing 100029, P.R. China

ARTICLE INFO

Article history:
Received 10 May 2008
Received in revised form 13 January 2010
Accepted 14 January 2010
Available online 25 January 2010

Keywords:
Chinese Altai
VMS deposit
Keketale Pb–Zn deposit
Back-arc basin

ABSTRACT

The Keketale Pb–Zn volcanogenic massive sulfide (VMS) deposit occurs in the early Devonian sequence of the Kangbutiebao Formation of the Southern Altai Metallogenic Belt (SAMB), northern Xinjiang, China. All the orebodies are stratabound and hosted by a suite of meta-sedimentary rocks intercalated with volcanic rocks. Major sulfide ores are pyrite, sphalerite, galena, with minor pyrrhotite and rare chalcopyrite. Massive, banded, and disseminated ores are the three main types. A typical VMS-type hydrothermal alteration zone is developed around the orebodies. Because of the overturned strata, an intense chlorite-, pyrite-rich crosscutting feeder zone is present immediately above the orebody. A sericite zone envelopes the chlorite zone. The meta-volcanic rocks show decoupled characteristics between the high field strength elements (Ta, Zr, and Hf) and large ion lithophile elements (Rb, Ba, and Th); all samples plot in the volcanic arc field in Ta *vs.* Yb discrimination diagrams. The $\delta^{34}S$ values of the stockwork zone are −1.0 to 4.5‰, and those of banded or massive ores range from −11.1 to −8.8‰, indicating that hydrothermal fluids may have had multiple sources and that bacterial sulfate reduction probably played an important role. Initial $(^{87}Sr/^{86}Sr)_i$ ratios and $\varepsilon_{Nd(t)}$ values of sulfide ores range from 0.70351 to 0.70951 and −3.6 to +3.0, respectively, whereas the corresponding values for wall rocks are 0.70560 to 0.70967 and −3.6 to +0.4. In a Sr–Nd isotopic correlation diagram, all the ores, meta-sedimentary rocks and volcanic rocks plot close to one another, clearly indicating a mixed mantle–crust source. Lead isotopic compositions of the ores are 17.995 to 18.232 for $^{206}Pb/^{204}Pb$, 15.498 to 15.669 for $^{207}Pb/^{204}Pb$ and 37.725 to 38.296 for $^{208}Pb/^{204}Pb$, with μ ($^{238}U/^{204}Pb$) ranging from 9.3 to 9.6. The Pb isotopes show a wide range in a Pb–Pb diagram, and the high $^{207}Pb/^{204}Pb$ values in the ores show distinctive crustal contamination signatures; a mixed mantle–crustal source is thus evident. Trace element geochemistry data are consistent with the Sr–Nd and Pb isotope data, and a subduction-related setting might be reasonable to account for this. Combining these observations with the local geology we further propose that the Keketale Pb–Zn deposit could have been formed in a back-arc (or an arc) basin.

1. Introduction

The Altaids is an important orogenic collage in Central Asia that hosts many world-class volcanogenic massive sulfide deposits (VMS), Cu–Ni deposits, gold deposits and other metallogenic types (e.g., Rui et al., 2002; Goldfarb et al., 2003; Zhang et al., 2009). Because of the complex geological setting and abundant mineral resources, the Altaids has attracted international attention during the past two decades (Coleman, 1989; Sengör et al., 1993; Windley et al., 2002; Xiao et al., 2004; Sun et al., 2008). Despite these extensive studies, there is no general agreement concerning its geological evolution and the geodynamic mechanisms involved. Sengör and Natal'in (1996) proposed that it is a "Turkic type" orogenic collage with a long, single arc, which was oroclinally bent in the middle to late Paleozoic, whereas Goldfarb et al. (2003) considered it as a Paleozoic, Cordilleran-style orogen. Windley et al. (2007) suggested that it is much more complex, and an archipelago-type (Indonesian) model is more viable. In particular, a temporal relationship between geodynamic processes and metallogeny is lacking; no individual, representative ore deposits have been related to these different models in either space or time up until now. For example, the tectonic settings of some ore deposits from the Chinese Altay Mountains, one important part of the southern Altaids, remain controversial. Whether these ore deposits formed in a continental margin, island arc, or back-arc setting is an issue that need to be tested by appropriate geodynamic models. Many researchers have studied the formation of the Altaids with respect to regional geology and the petrology and geochronology of contained geological units. Our systematical study of a representative Pb–Zn deposit (Keketale) in the Chinese Altay (Fig. 1) complements these studies and may help constrain the tectonic evolution of the Altaids, as well as understanding the geodynamic link between orogenic and ore-forming processes.

* Corresponding author. Key Laboratory of Mineral Resources, Institute of Geology and Geophysics, Chinese Academy of Sciences, P.O. Box 9825, Beijing 100029, P.R. China. Tel.: +86 10 82998520; fax: +86 10 62010846.
E-mail address: wanbo@mail.igcas.ac.cn (B. Wan).

0169-1368/$ – see front matter © 2010 Elsevier B.V. All rights reserved.
doi:10.1016/j.oregeorev.2010.01.002

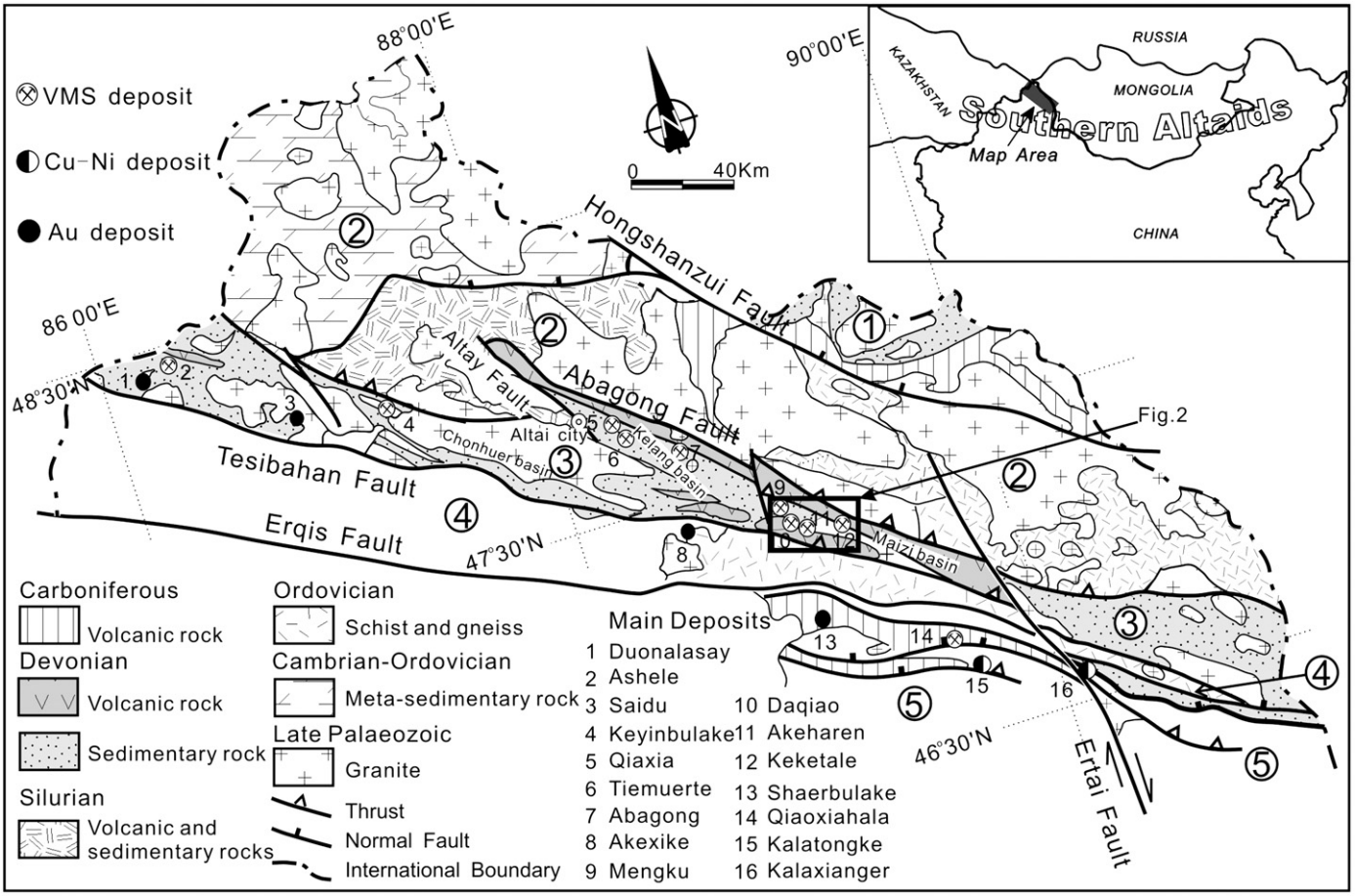

Fig. 1. Geological map of the Southern Altai Metallogenic Belt showing the main units and deposits. The location of Fig. 2 is marked. 1: Altaishan unit, 2: Halong unit, 3: Abagong unit, 4: Erqis unit, 5: Perkin–Ertai unit.

The Keketale deposit, the largest Pb–Zn deposit in the Chinese Altay, was discovered in 1986 and has been exploited since 1999. Although it has been studied for two decades, its geological setting and ore-forming mechanism are still highly debated. A continental margin rift setting (He et al., 1990; Chen et al., 1996), island arc setting (Windley et al., 2002), and back-arc setting (Wan and Zhang, 2006; Sun et al., 2008) have been proposed. Because the Keketale deposit is hosted by a suite of sedimentary rocks intercalated within rhyolitic volcanic rocks, and because its metallogenic setting was considered as continental margin rift in the last century, it is still debated whether it is a SEDEX- or VMS-type deposit. Wang et al. (1999) in fact, considered Keketale to be different from all other VMS deposits around the world and defined it as an "Altay type" deposit.

In this study, we attempt to address the above questions by a systematic trace element study including REE, and S–Sr–Nd–Pb isotopes, together with a reinterpretation of the regional tectonic setting. Our aim is to recognize the origin of the ore-forming materials, discuss the mechanisms of ore formation and characterize the tectonic setting of the Keketale deposit based on its geological and geochemical characteristics. We further aim to clarify whether it is a SEDEX- or VMS-type of deposit. Such information is not only the basis for understanding how a deposit may have formed, but is also very important as a guide for additional exploration in the Chinese Altay area.

2. Regional geology

The Altaids orogenic collage, which includes several mountain belts (e.g., the Mongol–Okhotsk, Altay–Sayan, Kazakhstan, Tianshan, and Urals), is surrounded by the East-European and Siberian Cratons to the north and is bordered by the Tarim and North China Cratons to the south (Sengör et al., 1993). The Chinese Altay belt is in the southern Altaids, straddling the international boundaries of China, Kazakhstan, and Russia; it is located at the southern edge of the Altay Mountains (Fig. 1, inset).

The Chinese Altay is divisible into five tectonics units (He et al., 1990; Windley et al., 2002; Xiao et al., 2004): (1) the Altaishan; (2) Halong; (3) Abagong; (4) Erqis; and (5) Perkin–Ertai (Fig. 1). These units are separated by a number of NW-striking faults; from north to south these are the Hongshanzui, Abagong, Tesibahan and Erqis faults. Most units developed by subduction-related processes and accreted in a southerly direction (based on present coordinates) from the Cambrian to the Permian. The Altaishan unit is dominated by mid–late Devonian andesites, dacites, and late Devonian to early Carboniferous shales, siltstones, greywackes, sandstones and limestones; the granitoids are mainly Carboniferous in age. The Halong unit is mainly composed of gneisses and schists, and is divisible into western low-grade Cambrian sediments, and eastern middle Cambrian felsic lavas and middle Ordovician to Silurian turbidites; the granitoids are mainly late Devonian. The Abagong unit is represented by late Silurian to early Devonian calc-alkaline lavas and pyroclastic rocks overlain by middle Devonian turbidities; the granitoids are mainly early Devonian and early Permian. The Erqis unit is a transcrustal strike–slip fault zone that consists of Ordovician to Silurian basalts, andesites and boninites, and Silurian to Devonian turbidites. The Perkin–Ertai unit comprises predominantly felsic-intermediate lavas and tuffs, andesitic and dacitic porphyries, and calc-alkaline granitic plutons, together with sandstones, conglomerates and limestones.

Table 1
Metal reserves and grade of the main VMS deposits in the Chonhuer–Abagong terrane.

Deposit	Reserve	Average grade	Location	References
Keketale	0.89 Mt Pb, 1.94 Mt Zn 650 t Ag	1.51 wt.% Pb, 3.16 wt.% Zn. 40 g/t Ag	Northern flank of Maizi syncline	Wang et al. (1999)
Akeharen	0.127 Mt. Pb, 0.5 Mt. Zn	2.89 wt.% Pb, 0.13 wt.% Zn.	Southern flank of Maizi syncline	Wang et al. (1999)
Daqiao	0.2 Mt Pb, 0.6 Mt. Zn.	0.29 wt.% Pb, 1.44 wt.% Zn.	Southern flank of Maizi syncline	Wang et al. (1999)
Mengku	220 Mt. Fe	43 wt.% Fe,	Northern flank of Maizi syncline	Wang et al. (2003)
Abagong	0.009 Mt Cu, 0.16 Mt Pb, 0.15 Mt Zn	0.09 wt.% Cu, 1.91 wt.% Pb, 3.49 wt.% Zn	Northern flank of Kelang syncline	Wang et al. (2003)
Tiemuerte	0.014 Mt Cu. 0.09 Mt Pb, 0.2 Mt Zn.	0.5 wt.% Cu, 1.39 wt.% Pb, 3.18 wt.% Zn	Northern flank of Kelang syncline	Jiang (2003)
Ashele	0.92 Mt Cu 0.48 Mt Zn	2.43 wt.% Cu 2.7 wt.% Zn	Southwestern part of Ashele basin	Chen (1990)

Precise isotopic ages of these units indicate that the whole orogen becomes progressively younger towards the south (Chen and Jahn, 2002; Windley et al., 2002; Wang et al., 2006; Sun et al., 2008). New whole-rock geochemical data indicate that the Altaishan, Halong and Abagong units formed in an active continental margin setting (Long et al., 2008; Sun et al., 2008). Among the 5 units, the Abagong unit hosts most of the volcanogenic massive sulfide (VMS) and orogenic gold deposits (e.g. Wang et al., 1999; Rui et al., 2002; Goldfarb et al., 2003). Because of its abundant mineral resources, we term the Abagong unit the Southern Altay Metallogenic Belt (SAMB) in this paper. This belt extends for 360 km along strike and is up to 70 km wide.

The SAMB hosts more than 30 major massive sulfide deposits and several smaller occurrences. Seven of these massive sulfide deposits (Keketale, Akeharen, Daqiao, Mengku, Abagong, Tiemuerte and Ashele; Fig. 1) have been mined for Cu, Pb, Zn and Fe for many years; tonnages and grades of these deposits are listed in Table 1; Keketale and Mengku are the largest. The SAMB is actually a polyphase fold system bounded by a series of faults and consists of four distinct volcanic sedimentary basins, which are from NW to SE: Ashele, Chonhuer, Kelang and Maizi. Each represents a giant syncline and hosts numerous VMS deposits or small occurrences; the largest number of deposits occurs in the Maizi basin. The Abagong and Tiemuerte deposits are located in the Kelang basin, whereas the Ashele deposit is found in the Ashele basin. The Keketale deposit is situated in the northern Maizi basin, whereas Mengku, Akeharen, and Daqiao occur in different sections of the Maizi basin (Fig. 2; Table 1).

From NW to SE, exposed strata in the Maizi basin consist predominantly of the early Devonian Kangbutiebao Formation, the middle Devonian Altai Formation, and a small part of the Silurian Kulumuti Group (Figs. 2 and 3). The Kulumuti group is represented by schists and sandstones, which constitute the basement of the Maizi basin, and which is uncomformably overlain by the Kangbutiebao Formation. The Kangbutiebao Formation consists of Devonian units with volcanic, pyroclastic and meta-sedimentary rocks and minor mafic volcanic rocks, and is 1 to 2 km thick. The Kangbutiebao Formation is the main ore-hosting stratum of the Keketale Pb–Zn deposit, together with other middle to large VMS deposits (Mengku, Akeharen and Daqiao). Zircon U–Pb dating of rhyolitic tuff just underlying the Keketale deposit gives a formation age of 407.3 ± 9.2 Ma (Zhang et al., 2000), which confirms the early Devonian age of the Kangbutiebao Formation and indicates that the mineralization time was slightly younger than 407 Ma. The middle Devonian Altay

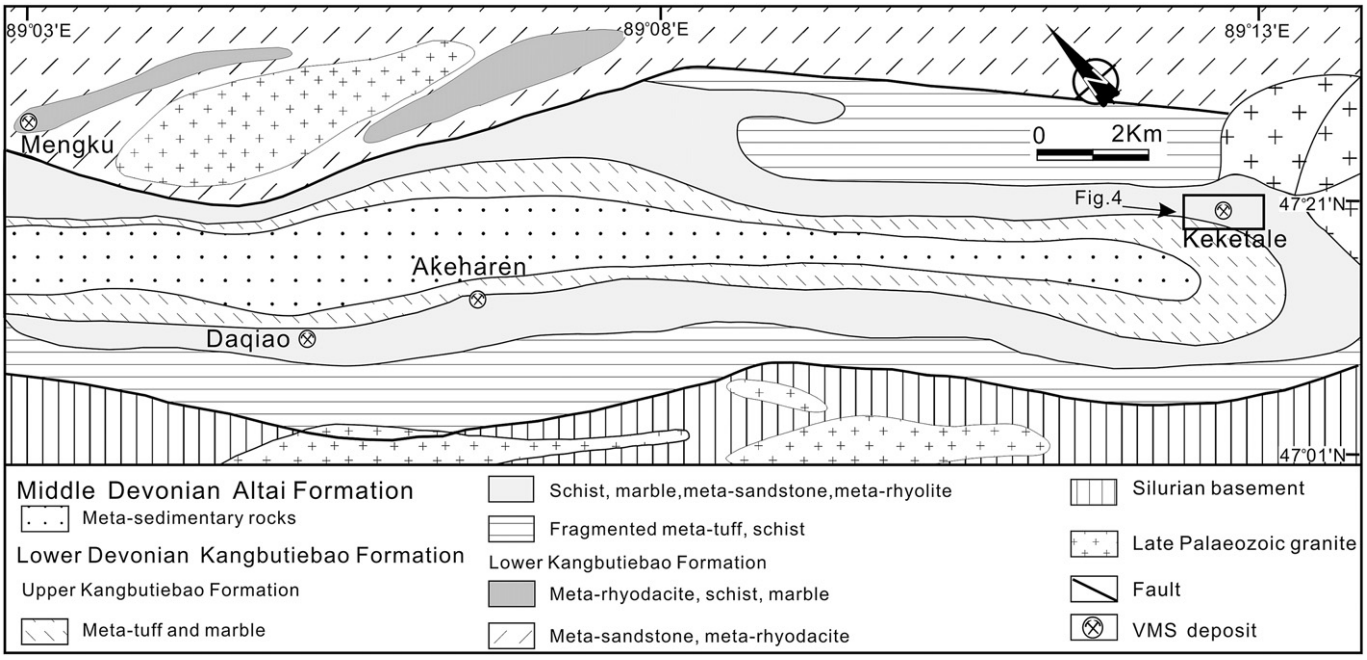

Fig. 2. Sketch map of the Maizi basin (after 706 Team of Northwest Metal Corp.). The location of Fig. 4 is marked.

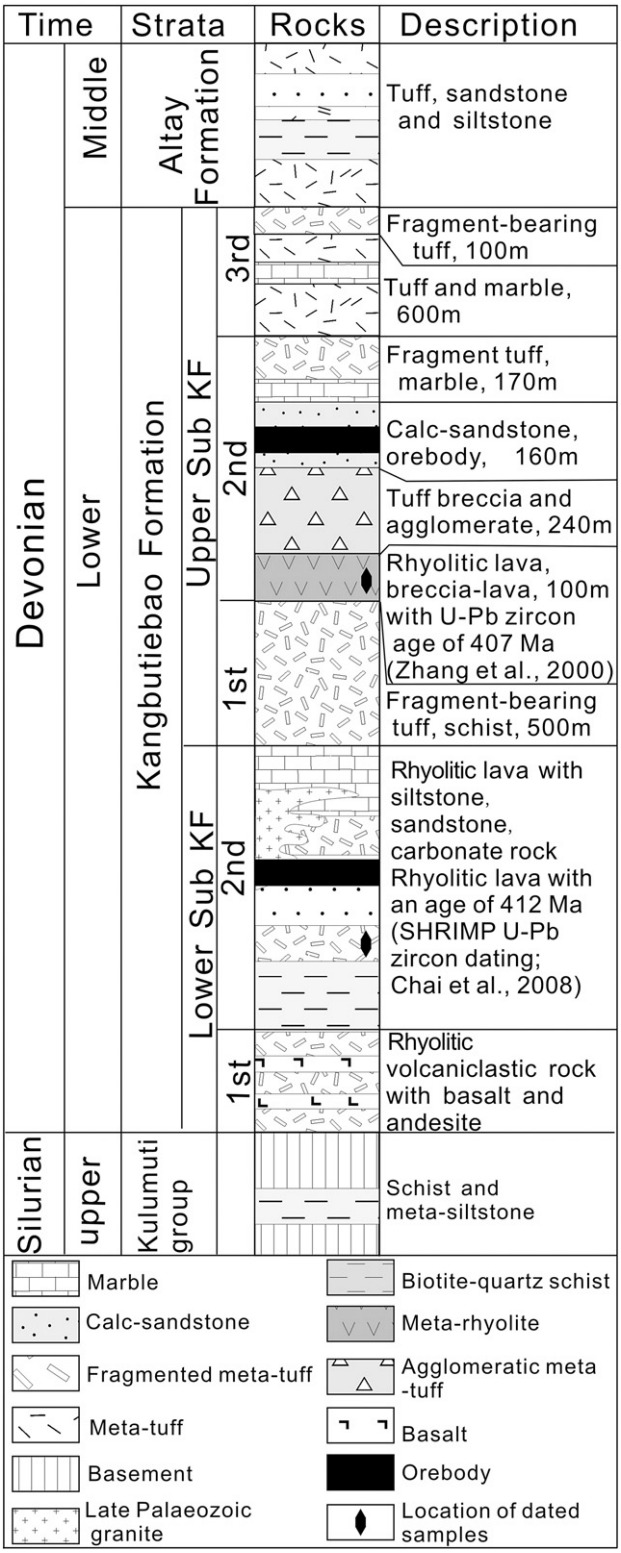

Fig. 3. Stratigraphic column for the Kangbutiebao Formation.

Formation overlies the Kangbutiebao Formation, and consists predominantly of a turbiditic sandstone–shale sequence together with minor basalts and siliceous volcanic rocks and it is well preserved in a low-grade metamorphic window.

At least 40% of the presently exposed area of the SAMB is occupied by intrusive rocks (Zou et al., 1988). Based on a compilation of reliable published ages of the Altay granites, Chen and Jahn (2002) suggested that the emplacement of granites occurred in two periods, 408 ~ 377 Ma (Zou et al., 1988; Chen and Han, 2006; Chen et al., 2006) and 344~290 Ma (Zou et al., 1988; Liu, 1990; Wang et al., 2006; Yuan et al., 2007). Despite their widespread occurrence elsewhere in the SAMB, intrusive rocks are not abundant in the Abagong unit. They are concentrated in its western and eastern segments of the belt and have U–Pb zircon ages that range from 290 to 390 Ma (Windley et al., 2002). Few intrusive rocks outcrop around the Keketale district, except for a swarm of pegmatitic quartz veins; they are unlikely to be related to the Keketale deposit.

Deformation fabrics in the Chinese Altai are divided into two main stages of development (Zhuang, 1994; Wei et al., 2007): stage one is characterized by tight to isoclinal folds, inferred to have developed in the late Devonian; stage two is dominated by strike–slip structures that are interpreted as having developed in the Permian to Triassic (Laurent-Charvet et al., 2002).

3. Geology of the Keketale Pb–Zn deposit

The Keketale deposit is the largest and most important economic producer of Pb and Zn in the SAMB. It consists of 12 orebodies that outcrop over an area of nearly 0.7 km^2. Total Pb + Zn metal reserves are ca. 3 million tonnes; the No.7 and 9 orebodies account for almost 70% of this total. Other elements of economic interest include Ag which has an average grade of 19.7 g/t.

The deposit is situated in the northern Maizi basin, a giant overturned syncline with an axial plane that dips NE and strikes NW–SE (Fig. 3). Exposed strata in the Keketale mine district belong to the upper part of the Lower Devonian Kangbutiebao Formation (Fig. 4). All the orebodies at Keketale are located in the overturned limb of the syncline, striking NW and dipping SE like the host strata. They are hosted by meta-calc-sandstones, and interlayered with meta-rhyolitic rocks. The structural footwall to the SE of the deposit is mainly fragmented meta-tuff, and the structural hanging wall to the NW of the deposit is mainly meta-rhyolite, agglomeratic meta-tuff and meta-tuff. All the orebodies vary considerably in size, from more than 700 m in length, 80 m in thickness and down-dip extent of 500 m (No. 7 orebody), to less than 100 m in length, 10 m thickness and a down-dip extent of 200 m. Because the No. 7 orebody has the largest reserves of the Keketale ore deposits, we show here a profile across it (Fig. 5).

The No. 7 orebody includes one main lens and several smaller lenses. All the lenses are stratabound within the meta-calc-sandstone of the upper Kangbutiebao Formation. The main lens of the No. 7 orebody is slightly lenticular, but it is apparently elongated down the dip direction. The deformation responsible was probably the same as that which folded the host strata. The fact that the No. 7 orebody is apparently more deformed than other orebodies, may be a consequence of its specific structural position close to the hinge of the overturned syncline. The main lens at Keketale has been oxidized at surface; an oxide zone extends from the surface to a depth of 20 m, although all the lenses extend down to about 550 m depth. The main lens is dominated by massive ore (sulfide minerals amount to >60 vol.%; Fig. 6), but banded ores, laminated ores and disseminated ores are also common especially in the margin of the ore lens. The disseminated ores are very common in the uppermost part of the lens and even in the overlying calcareous meta-sandstone. In the immediate hanging wall of the main lens there are several vein-type ores. We consider that the disseminated and vein-type ores together represent the feeder zone of a sub-seafloor hydrothermal system. The smaller lenses in the footwall of the main lens mainly consist of massive ore with very high metal grades up to 8.5% combined (Pb + Zn).

The main sulfide minerals in decreasing order of abundance are pyrite, sphalerite, galena and pyrrhotite, with minor chalcopyrite. Gangue minerals are quartz, calcite, biotite and plagioclase. Pyrrhotite and chalcopyrite have a xenomorphic texture, are always associated

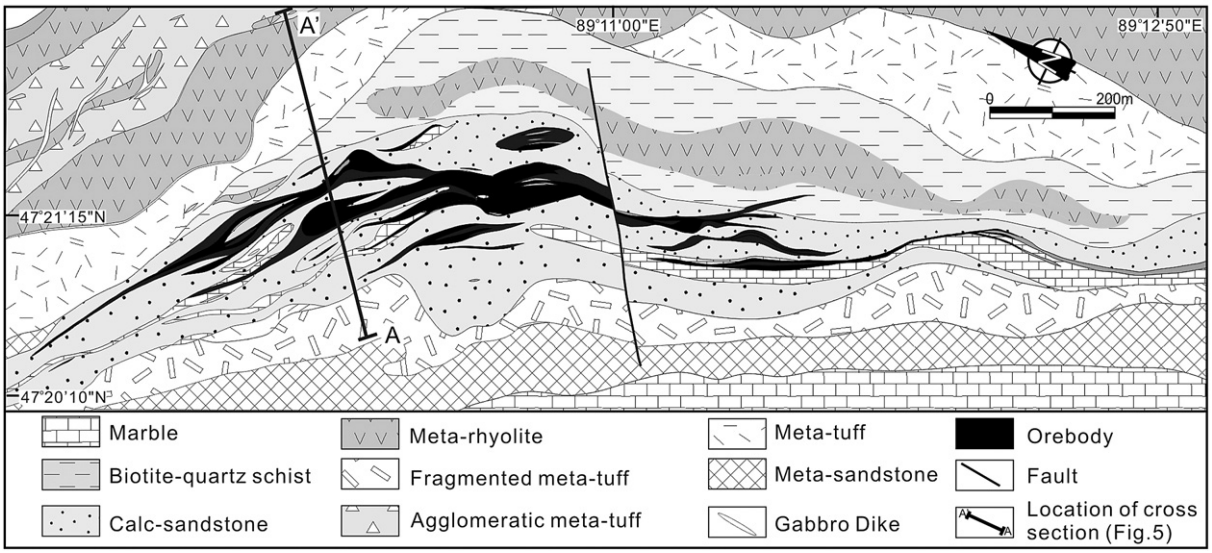

Fig. 4. Geologic map of the Keketale Pb–Zn deposit (after 706 Team of Northwest Metal Corp.). The location of cross-section *A*–*A*′ (Fig. 5) is indicated.

with vein-type pyrite, and are located in the uppermost part of the main lens. Pyrite occurs as idiomorphic grains and hypidiomorphic granular aggregates throughout the complete extent of the lenses. Sphalerite and galena are two most important economic minerals in the Keketale deposit. Sphalerite mostly occurs as xenomorphic aggregates, sometimes as the matrix to pyrite grains, and mainly in the upper and middle parts of the ore lens. Galena mainly occurs as idiomorphic grains and sometimes as the interstitial phase amongst many other sulfides (e.g., pyrite, sphalerite), and it is located in the middle and lower part of the lens. The Pb/Zn ratio thus increases with depth. Based on the above description, a general metal zonation can be described: (Fe + Cu) in the uppermost parts of No. 7 orebody, (Fe + Zn + Pb; Zn > Pb) in the middle

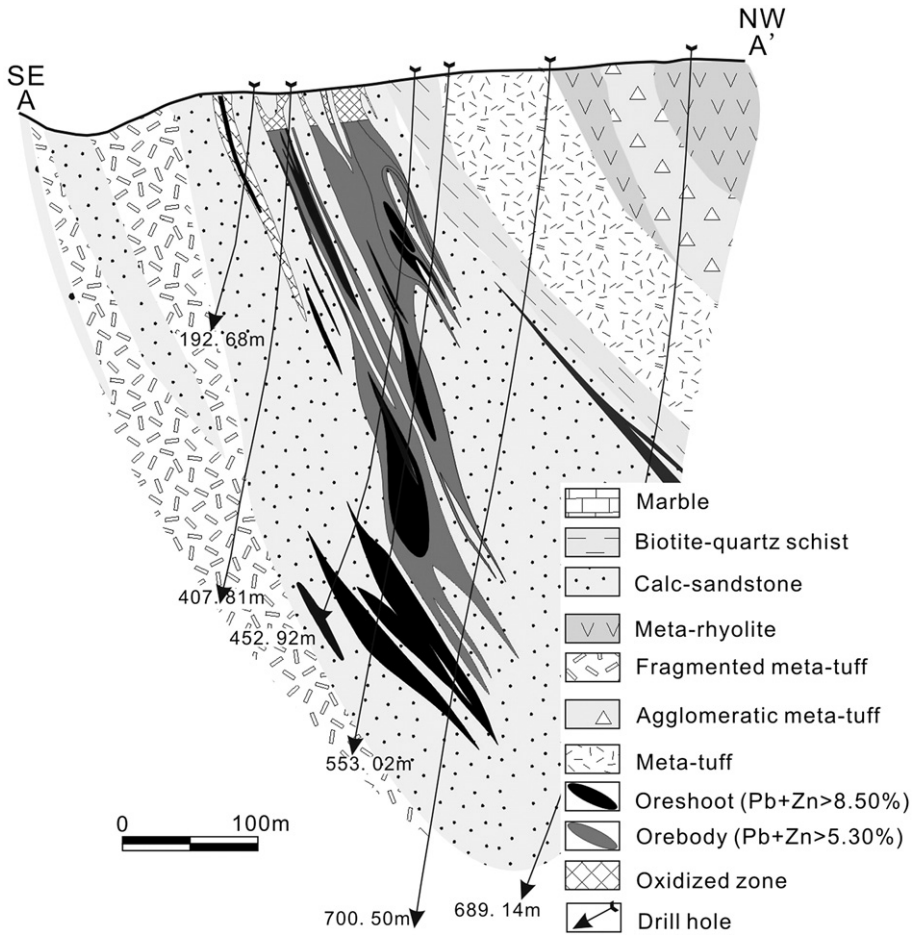

Fig. 5. Geological cross-section, *A*–*A*′ (see Fig. 4), in the Keketale Pb–Zn deposit (after 706 Team of Northwest Metal Corp.). Stratigraphic units are overturned with polarity to the NE.

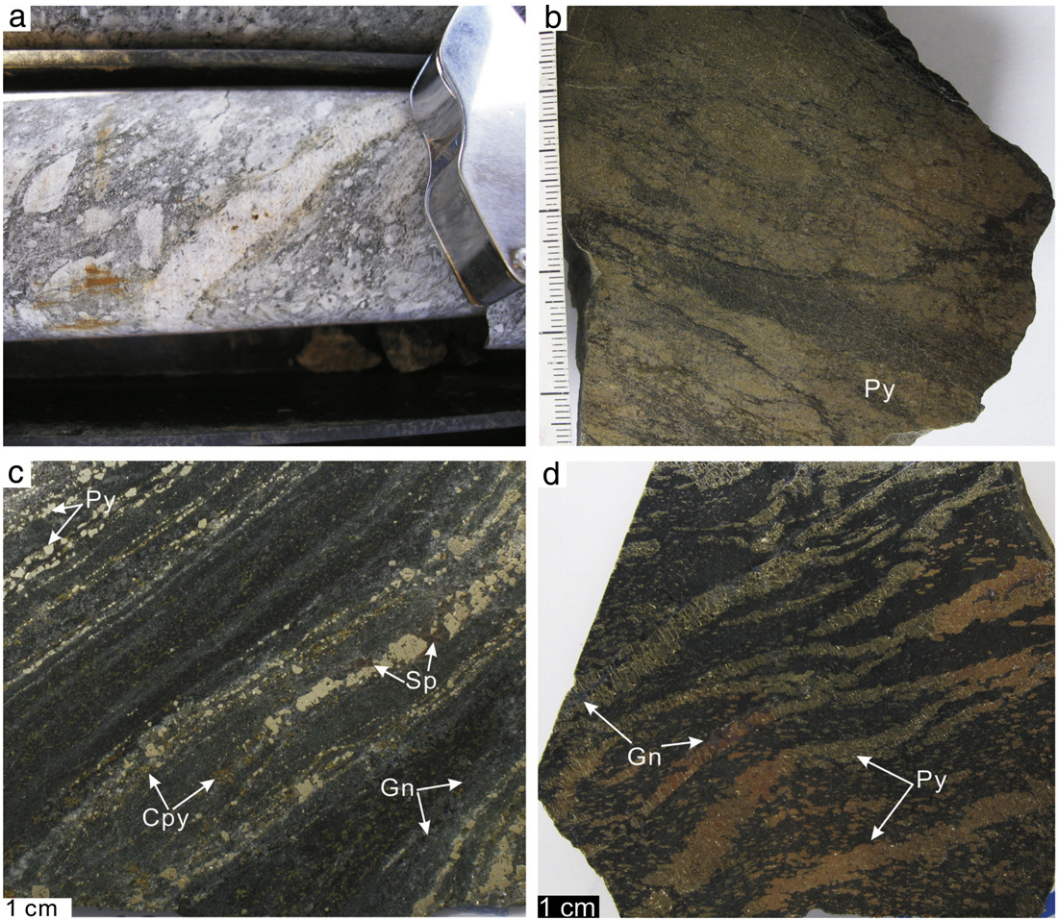

Fig. 6. Textures of volcanic rocks and ores from the Keketale deposit. (a) Underlying rhyolitic rocks. (b) Massive ores. (c) Banded ores [pyrite (Py) + galena (Gn) + sphalerite (Sp) + chalcopyrite (Cpy)] in a siliceous host rocks. (d) Banded ores (pyrite + galena) affected by later deformation.

of the orebody, and (Fe + Pb + Zn; Pb > Zn) at the base of the orebody. Chalcopyrite is very minor and has no economic importance in the Keketale deposit.

Hydrothermal alteration in the rocks surrounding VMS deposits is a common phenomenon (Franklin et al., 1981) which has attracted much attention. Study of alteration zones provides supplementary

Table 2
REE and trace elemental compositions (ppm) of country rocks in the Keketale Pb–Zn deposit.

No.	MZ43	MZ51	MZ57	Mz59	MZ44	MZ46	MZ45	MZ55	MZ58
Name	Marble	Schist	Meta-sandstone		Meta-rhyolitic tuff		Meta-rhyolite		
La	2.77	47	32	11	35	24	28	40	27
Ce	5.28	93	64	26	75	57	58	80	55
Nd	3.11	42	28	14	34	29	31	39	28
Sm	0.58	8.22	5.62	3.51	6.21	6.3	5.93	8.19	6.57
Eu	0.10	1.38	0.6	0.60	1.26	1.14	1.07	1.15	1.22
Gd	0.55	5.67	4.26	4.06	6.39	6.91	5.02	8.21	5.21
Tb	0.09	1.07	0.72	0.79	1.12	1.29	0.81	1.49	0.84
Ho	0.09	1.5	1.13	1.19	1.5	1.69	1.09	2.04	1.15
Tm	0.04	0.62	0.47	0.53	0.59	0.65	0.42	0.91	0.55
Yb	0.27	3.88	3.13	3.4	3.46	3.8	2.64	5.59	3.36
Lu	0.04	0.63	0.49	0.51	0.52	0.49	0.44	0.83	0.52
Eu/Eu*	0.6	0.61	0.42	0.52	0.61	0.53	0.58	0.42	0.62
La/Yb	10.3	12.1	10.2	3.23	10.1	6.32	12	10.3	10
∑REE	13	204	140	66	165	132	134	187	129
Sr	207	107	50.9	32.3	68	25	52	56	24
K	39	16,200	17,100	11,300	19,500	5900	26,400	16,500	24,700
Rb	2.52	98	180	142	86	50	65	47	30
Ba	16.9	480	661	1260	340	120	370	270	380
Th	0.18	13	21	14	12	13	8.41	8.45	7.56
Ta	0.18	1.20	1.22	1.00	1.20	1.01	0.74	0.88	1.04
Zr	11	220	95	50	170	82	105	181	56
Hf	0.04	5.97	5.58	4.30	4.58	3.02	3.14	5.21	2.12

$Eu/Eu^* = Eu_N/(Sm_N \times Gd_N)^{1/2}$.

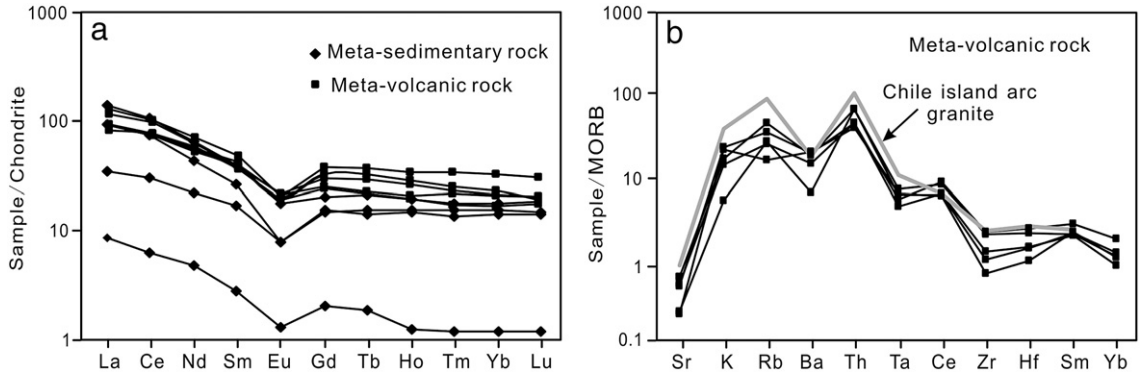

Fig. 7. Chondrite-normalized REE patterns of (a) country rocks and (b) MORB-normalized spider diagram for the volcanic rocks from the Keketale Pb–Zn deposit. Chondrite REE compositions from Boynton (1984); MORB compositions and Chile island granite from Pearce et al. (1984).

information about the chemical and thermal nature of fluids, as well as the extent and geometry of hydrothermal systems. Strong hydrothermal alteration also occurs in the immediate vicinity of the ore lens at Keketale (Qin et al., 1998). Hydrothermal alteration in this deposit includes a chlorite zone, a sericite zone, carbonatisation, pyritization and skarnification. An intense chlorite zone, characterized by chlorite ± pyrite ± quartz ± carbonate, occurs immediately above the ore lenses (because of the overturned strata) both in calc-sandstone and in rhyolitic tuff. In this chlorite zone, there is evidence of pyritization, and skarn formation, which occurs in a narrow stratiform sheet immediately below the ore lenses. The skarns result from interaction between a hydrothermal fluid and marbles and the calcareous meta-sedimentary rocks. Enveloping the inner chlorite zone is a broad sericite zone characterized by sericite ± chlorite ± carbonate. This mainly occurs in the meta-rhyolite, and to a minor extent in sedimentary rocks.

4. Geochemistry of the Keketale Pb–Zn deposit

4.1. Sample description and effects of alteration

All samples studied were collected in the Keketale mine area (long. E89°09′54″–89°13′00″, lat. N47°20′06″–47°22′38″). Massive, banded sulfide ores were collected from the middle and lower parts of the main ore lens of the No. 7 orebody, and disseminated pyrite from uppermost part of the main ore lens. Volcanic and sedimentary rocks were collected far from the orebody to avoid possible effects of hydrothermal alteration. However, as mentioned above, the rocks have undergone at least two stages of deformation. The volcanic and sedimentary rocks at Keketale have been regionally metamorphosed to greenschist facies based on the simple metamorphic mineral assemblage of chlorite + quartz + biotite in most rocks. Therefore, our study focuses on sulfur isotopes of sulfides to discuss the origin of the ore-forming fluids, because the sulfur isotopes should not be significantly affected by low-temperature metamorphism (Huston, 1999). We also compare the Sr, Nd and Pb isotope systematics between those of the sulfide ores and country rocks to determine whether the ore-forming fluids were derived from the surrounding rocks or not. Furthermore, we use some trace elements in order to discuss the tectonic setting of the volcanic rocks, and later their metallogenic setting.

4.2. Analytical methods

All elemental and isotopic measurements were carried out at the Institute of Geology and Geophysics, Chinese Academy of Sciences (IGGCAS). Trace elements were determined with a VG-PQII ICP-MS, using indium as an internal standard to correct for matrix effects and instrument drift. Sulfur isotopes were determined with a MAT 252 isotope ratio mass spectrometer. Sulfide samples were combusted in the presence of excess CuO in a vacuum to produce SO_2. The precision of analysis is better than 0.3‰, and the values are reported relative to the Canyon Diablo Troilite (CDT). Sr, Nd and Pb separation from sulfide samples followed the procedures described by Chen et al. (2007). Isotopic compositions of these elements were measured on a Finnigan MAT-262 mass spectrometer at IGGCAS. Thermal mass fractionation of Sr and Nd isotopes was corrected with a power law and $^{86}Sr/^{88}Sr = 0.1194$ and $^{146}Nd/^{144}Nd = 0.7219$, respectively. Repeat analyses of the NIST-987 reference material yielded $^{87}Sr/^{86}Sr = 0.710253 \pm 0.000010$ ($N = 8$, 2σ) and for the La Jolla standard $^{143}Nd/^{144}Nd = 0.511862 \pm 0.000009$ ($N = 8$, 2σ). Pb was separated from the sulfides by anion exchange chromatography using a HBr–HCl cleaning-elution procedure. Five analyses of reference material SRM 981 yielded $^{206}Pb/^{204}Pb = 16.916 \pm 0.009$ (2σ), $^{207}Pb/^{204}Pb = 15.461 \pm 0.010$ (2σ), $^{208}Pb/^{204}Pb = 36.616 \pm 0.012$ (2σ).

4.3. Trace element geochemistry

Normalized trace element contents, including rare earth elemental compositions, are listed in Table 2 and plotted in Figs. 7 and 8. REE patterns for meta-sedimentary and -volcanic rocks are overall similar, showing fractionated LREE and flat HREE patterns. They also display distinct Eu negative anomalies ($Eu/Eu^* = 0.55$; Fig. 7a). In general, the meta-volcanic rocks have higher REE contents than the meta-sedimentary rocks. The underlying meta-volcanic rocks show decoupled characteristics between high field strength elements (HFSE) and large ion lithophile elements (LILE) (Fig. 7b). HFSE, Ta Zr, Hf, and Yb are depleted relative to LILE, and the distribution patterns

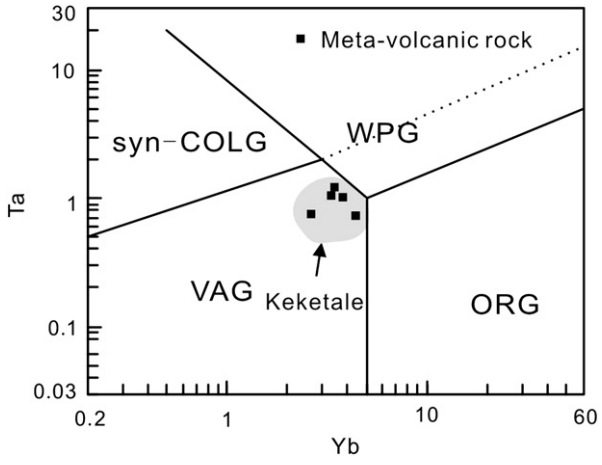

Fig. 8. Tectonic discrimination diagrams after Pearce et al. (1984). (a) Ta *vs.* Yb. Grey field from Cong et al. (2007).

Table 3
Sulfur isotopes of sulfide ores from Keketale Pb–Zn deposit.

Sample no.	Mineral	Description	δ^{34}S‰
MZ08	Py	Disseminated ores in sericitized sandstone	0.2
MZ15	Py	Disseminated ores in sericitized sandstone	1.8
MZ19	Sp	Disseminated ores in sericitized schist	1.9
MZ23-1	Po	Disseminated ores in sericitized sandstone	4.5
MZ24-1	Py	Disseminated ores in chloritized sandstone	3.9
MZ25-2	Sp	Disseminated ores in chloritized sandstone	3.7
MZ27	Py	Disseminated ores in chloritized schist	−1.0
MZ36	Po	Disseminated ores in meta-tuff	−0.6
MZ38	Py	Disseminated ores in chloritized sandstone	1.9
MZ39	Py	Disseminated ores in chloritized tuff	3.7
MZ40	Py	Disseminated ores in the main ore lens	−9.0
MZ41	Py	Banded ore in the main ore lens	−9.3
MZ42	Sy	Massive ore in the main ore lens	−11.1
MZ47	Gn	Massive ore in the main ore lens	−8.8

Abbreviation: Po–pyrrhotite; Py–pyrite; Gn–galena; Sp–sphalerite.

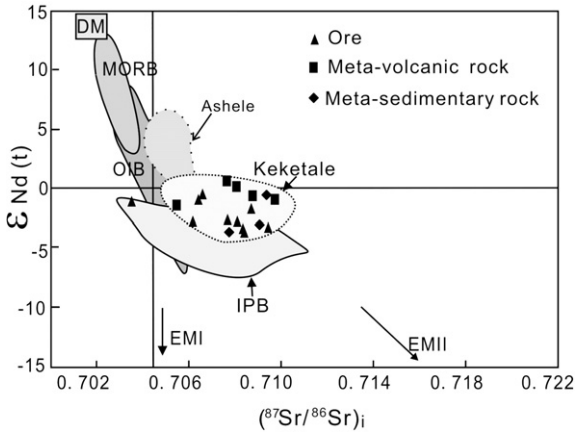

Fig. 9. Sr–Nd isotope correlation plot of sulfide ores and wall rocks in the Keketale deposit. DM (Deplete Mantle), MORB (Mid-Ocean ridge basalt), OIB (Ocean island basalt), EMI (Enriched Mantle 1), EMII (Enriched Mantle 2) from Zindler and Hart (1986); Ashele data from Wan et al. (2010); IPB data see compilation in Tornos et al. (2005).

are similar to those of felsic igneous rocks from an island arc setting (Chile island arc granites; Pearce et al., 1984). The Ta/Yb ratio is low, so the samples plot in the volcanic arc field of the diagram. Cong et al. (2007) made a geochemical study of the meta-volcanic rocks of the Kangbutiebao Formation, which hosts the VMS deposits in the SAMB. They used Nb/Y ratios to decipher the volcanic forming setting and plotted all samples in the volcanic arc setting field (Fig. 8). Our results, in this study, are consistent with those of Cong et al. (2007), in that they also suggest that the volcanic rocks formed in a island arc setting.

4.4. Isotope geochemistry

4.4.1. Sulfur isotopes

We have focused on sulfides from the underlying hydrothermal feeder zone. The sulfur isotope compositions of ores are listed in Table 3. The ores have a wide variation of δ^{34}S‰ ranging from −11.1‰ to 4.5‰ that can be separated into two groups according to their structural position in the orebody. The disseminated sulfides in the immediate vicinity of the ores have a very limited variation of δ^{34}S ranging from −1.0‰ to 4.5‰. Disseminated pyrite in the sericite zone has δ^{34}S values of 0.2 to 3.9‰, and the δ^{34}S values of disseminated sphalerite and pyrrhotite in the sericite zone are 1.9 and 4.5‰, respectively. Disseminated pyrite in the chlorite zone has δ^{34}S values of −1.0 to 3.7‰, and the δ^{34}S values of disseminated sphalerite and pyrrhotite in the chlorite zone are 3.7 and −0.6‰, respectively. Based on the above data, the sulfides in the hydrothermal zones representing the feeder zones have a δ^{34}S close to 0‰. In contrast, the δ^{34}S values of sulfides in the main ore lens range from −11.1 to −8.8‰. Disseminated pyrite in the main ore lens has a δ^{34}S of −9.0‰, and pyrite from the banded ores has a δ^{34}S of −9.3‰. Sphalerite and galena from massive ores have δ^{34}S values of −11.1 and −8.8‰, respectively. The sulfides in the main ore lens have very light sulfur isotopic ratios, which are clearly distinct from those in the feeder zones.

4.4.2. Sr–Nd–Pb isotopes

The Rb–Sr and Sm–Nd isotopic compositions of 10 sulfide ores (4 pyrite ores, 5 sphalerite ores), 3 meta-sedimentary rocks and 5 volcanic rocks are listed in Table 4. The ages of the underlying volcanic rocks and the pyrites from the ores are 407 ± 9.2 Ma (U–Pb zircon; Zhang et al., 2000) and 373 ± 37 Ma (Rb–Sr isochron of sulfide; Li and Chen, 2004), respectively. Based on the stratabound characteristics of the orebodies, a model age of 400 Ma is used here to calculate the initial ^{87}Sr/^{86}Sr ratios and $\varepsilon_{Nd(t)}$ of the sulfide ores and

Table 4
Sr–Nd isotopic compositions of ores and rocks from Keketale Pb–Zn deposit.

	Sample	Rb	Sr	^{87}Rb/^{86}Sr	^{87}Sr/^{86}Sr	2σ	$(^{87}Sr/^{86}Sr)_i$	Sm	Nd	^{147}Sm/^{144}Nd	^{143}Nd/^{144}Nd	2σ	$\varepsilon_{Nd(t)}$
KT1-4[a]	Sphalerite	0.12	19.57	0.018	0.708450	20	0.708398	1.0200	3.5200	0.1763	0.512437	16	−3.6
KT1-5[a]	Sphalerite	0.23	38.23	0.018	0.708360	30	0.708300	0.9500	4.3400	0.1326	0.512346	18	−3.3
KT1-6[a]	Sphalerite	0.19	9.22	0.059	0.708970	50	0.708663	1.3200	5.8500	0.1366	0.512358	13	−1.6
KT1-7[a]	Sphalerite	0.36	45.99	0.022	0.708220	20	0.708074	0.8700	3.3100	0.1588	0.512407	25	−2.7
KT1-8[a]	Pyrite	1.40	4.59	0.883	0.712710	20	0.707673	0.0600	0.3100	0.1162	0.512294	20	−2.5
KT1-11[a]	Sphalerite	4.21	2.77	4.392	0.725510	70	0.706181	0.3000	2.2300	0.0812	0.512210	14	−2.6
MZ47-1	Pyrite	0.08	9.44	0.025	0.706750	15	0.706559	0.0350	0.1866	0.1135	0.512444	20	−0.4
MZ42-1	Pyrite	0.72	2.23	0.946	0.714873	16	0.709514	0.0450	0.1144	0.2377	0.512876	15	3.0
MZ45-1	Pyrite	12.49	10.97	3.299	0.722298	15	0.703511	0.0482	0.1771	0.1647	0.512537	16	−1.1
MZ45-2	Pyrite	2.37	4.44	1.551	0.715103	15	0.706267	0.0160	0.0808	0.1199	0.512360	18	−0.7
BJ98-14[b]	Schist	47.4	382	0.358	0.711418	7	0.709379	4.3600	20.6000	0.1281	0.512436	8	−0.4
BJ98-09[b]	Schist	128	186	1.988	0.720367	8	0.709043	4.7500	23.8300	0.1205	0.512284	8	−3.0
BJ98-07[b]	Schist	151	46	9.303	0.743638	7	0.707735	5.7500	28.4200	0.1223	0.512260	8	−3.6
MZ59	Meta-tuff	102	49	6.060	0.749870	13	0.709685	3.6592	13.7503	0.1609	0.512482	13	−0.9
MZ48	Meta-tuff	0.35	46	0.022	0.708917	11	0.708775	6.6346	26.0573	0.1539	0.512524	12	−0.5
AL9[c]	Meta-rhyolitic lava	9.38	32	0.846	0.712977		0.708161	7.1000	34.2000	0.1473	0.512504		−0.1
AL12[c]	Meta-tuff breccia	6.61	42	0.433	0.720153		0.707851	4.0500	20.3000	0.1282	0.512351		0.4
AL20[c]	Meta-rhyolitic lava	160	78	6.069	0.740167		0.705597	5.8400	25.4000	0.1543	0.512439		−1.7

Initial ^{87}Sr/^{86}Sr and $\varepsilon_{Nd(t)}$ values were calculated for an age of 400 Ma. Other parameters: $^{143}Nd/^{144}Nd_{CHUR(0)} = 0.512638$, $^{147}Sm/^{144}Nd_{CHUR(0)} = 0.1967$, $\lambda^{87}Rb = 1.42 \times 10^{-11}$ a^{-1}, $\lambda^{147}Sm = 6.54 \times 10^{-12}$ a^{-1}.

[a] Li and Chen (2004).
[b] Chen and Jahn (2002).
[c] Cong et al. (2007).

Table 5
Pb isotope composition of ores and rocks from Keketale Pb–Zn deposit.

Sample no.	Name	$^{206}Pb/^{204}Pb$	$^{207}Pb/^{204}Pb$	$^{208}Pb/^{204}Pb$	μ
MZK7-6[a]	Galena	18.135	15.634	38.150	9.56
MZK7-2[a]	Pyrite	18.015	15.515	37.725	9.34
Zk15-7-26[a]	Pyrite	18.109	15.589	37.960	9.48
B-6[a]	Galena	18.049	15.541	37.820	9.48
M7-7[a]	Galena	18.114	15.607	38.058	9.53
T88455[a]	Galena	17.959	15.496	37.610	9.31
MZ47-1	Pyrite	18.089	15.572	37.918	9.44
MZ42-1	Pyrite	18.059	15.567	37.911	9.44
MZ45-1	Pyrite	18.182	15.662	38.180	9.61
MZ45	Pyrite	18.045	15.533	37.812	9.37
MZ59	Meta-tuff	18.232	15.669	38.296	9.62
MZ48		18.122	15.572	37.963	9.44
Kkp3[b]		18.113	15.539	38.132	9.38
Kkp5[b]		18.277	15.580	38.108	9.44
Kkp6[b]	Schist	18.065	15.583	37.937	9.47
Kkp7[b]	Marble	18.243	15.554	38.062	9.39
Kkp8[b]	Marble	18.282	15.551	38.157	9.38

[a] Wang et al. (1998).
[b] Zhang et al. (2000).

the country rocks. The initial $^{87}Sr/^{86}Sr$ ratios of sulfide ores in the orebodies range from 0.70351 to 0.70951; $\varepsilon_{Nd(t)}$ values range from −3.6 to −0.4. The initial $^{87}Sr/^{86}Sr$ ratios and $\varepsilon_{Nd(t)}$ values of the meta-sedimentary rocks are 0.70774 to 0.70938 and −3.6 to −0.4, respectively. Corresponding values in the underlying volcanic rocks are 0.70444 to 0.74987 and −1.7 to +0.4, respectively (Fig. 9).

Pb-isotopic ratios of the ores range from 17.959 to 18.182 for $^{206}Pb/^{204}Pb$, 15.496 to 15.662 for $^{207}Pb/^{204}Pb$ and 37.610 to 38.180 for $^{208}Pb/^{204}Pb$. The ratios from meta-sedimentary rocks and volcanic rocks range from 18.065 to 18.282 for $^{206}Pb/^{204}Pb$, 15.539 to 15.669 for $^{207}Pb/^{204}Pb$ and 37.937 to 38.296 for $^{208}Pb/^{204}Pb$. All samples have a narrow range of μ values (calculated with respect to a single-stage model), between 9.3 and 9.6 (Table 5). Fig. 10a shows that the Pb isotope compositions from the ores form an array at a high angle to the "orogen" curve, with most data close to the orogen curve for Phanerozoic Pb (Ma et al., 2004). The array spreads from values typical of the mantle reservoir to values more radiogenic than the upper crustal reservoir (Zartman and Doe, 1981). In Fig. 10b, the Pb isotope data from the ores form an array with distinct $^{208}Pb/^{204}Pb$ enrichment, suggesting that lead in the ores was derived from a mixed mantle–crust reservoir.

5. Discussion

The ore-forming mechanism and the tectonic setting of the Keketale Pb–Zn deposit are still highly debated. We have used trace elements, stable and radiogenic isotope data, in combination with a reinterpretation of the regional tectonic setting, to characterize the sources of ore-forming materials, the mineralization mechanism and the tectonic environment.

5.1. Source of ore-forming materials

Previous sulfur isotope studies of the Keketale deposit showed a very wide range between −15.8 and 5.8‰ (Wang et al., 1998; Fig. 11); our sulfur isotope data are consistent with previous results. However, we focus on different isotopic systematics between the hydrothermal feeder zones and the main orebodies. Disseminated sulfide ores from the originally underlying alteration zone, which is in immediate vicinity to the ores, have sulfur isotopic compositions with an average value of 2.3‰ (−1.0 to 4.5‰), different those from the main ore lens (average value of −9.5‰; range −11.1 to −8.8‰) (Fig. 11). The large difference in sulfur isotopic values between the hydrothermal feeder zone and the main orebody may indicate that the sulfur originated from different sources. The total range is not unlike that of normal marine sediments (Ohmoto and Rye, 1979), except for the lack of more positive values, and they may indicate a significant contribution of sulfur produced by biologic seawater sulfate reduction. The $\delta^{34}S$ values of the hydrothermal feeder zone sulfides can be explained as magmatic, either via leaching of magmatic sulfides or directly from magma degassing (Velasco et al., 1998), and the very negative value in the main orebody could indicate biogenic sulfur. Our result is consistent with the Tharsis deposit in the Iberian Pyrite Belt (IPB), where the average sulfur compositions of the stockwork zone and main orebodies are around −0.3‰ and −6.4‰, respectively (Tornos et al., 2008). With respect to the Keketale deposit, however, the amount of sulfide in the underlying alteration zone is much less than that in the main ore lens, hence the main ore-forming sulfur should originate from biogenesis.

We compare the sulfur isotopic compositions of the SAMB and IPB VMS deposits. Compilations of S isotope values from the literature show that the $\delta^{34}S$ values of deposits in the whole SAMB extend over a wide range from −23.2 to +14‰ (Ye et al., 1997; Wang et al., 1999; Jiang, 2003; Wang et al., 2003), and are similar to values of IPB

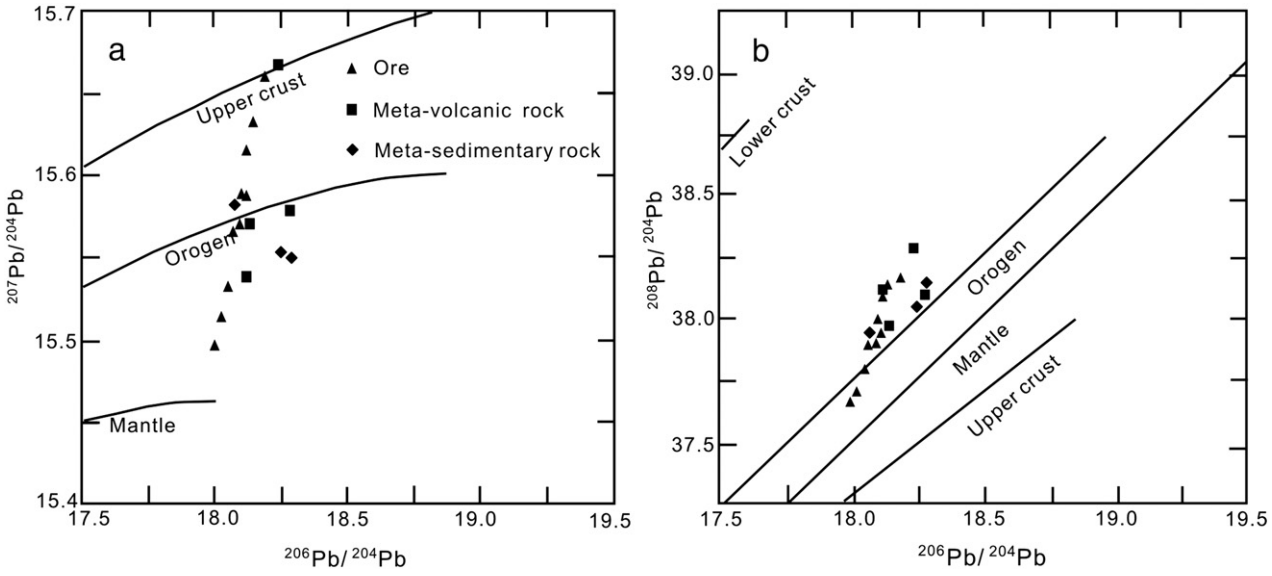

Fig. 10. Pb isotope composition of sulfide and rocks from the Keketale deposit. (a) $^{207}Pb/^{204}Pb$ *vs.* $^{206}Pb/^{204}Pb$. (b) $^{208}Pb/^{204}Pb$ *vs.* $^{206}Pb/^{204}Pb$. After Zartman and Doe (1981).

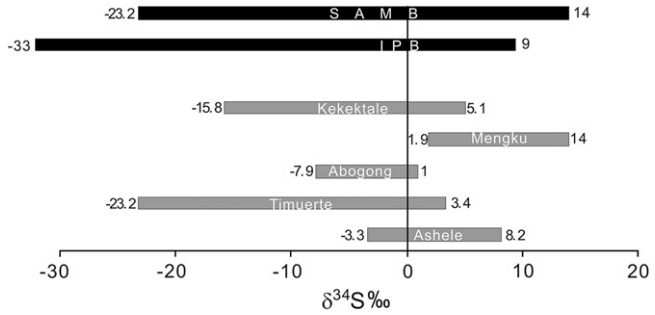

Fig. 11. Sulfur isotope composition of selected volcanogenic massive sulfide deposits from the SAMB. $\delta^{34}S$ value in Ashele from Ye et al. (1997), Abagong from Jiang (2003), Keketale from Wang et al. (1999) and this study, Tiemuerte from Wang et al. (1999), Mengku from Wang et al. (2003), IPB see compilation in Tornos et al. (2008).

(−33‰ to 9‰; see compilation in Tornos et al., 2008; Fig. 10). Most authors agree that the sulfur was derived from seawater, with bacterial activity accounting for the negative values. In this study, we notice the difference between the underlying alteration zone and the main orebodies. Since the deposits in the IPB have a similar range as in the SAMB, we agree with previous explanations that the sulfur was either leached from underlying rocks, was derived from bacterial reduction of seawater sulfate, or by a combination of these two processes (Tornos, 2006; Tornos et al., 2008).

The initial $^{87}Sr/^{86}Sr$ ratio of most sulfide ores ranges from 0.706181 to 0.709514, and $\varepsilon_{Nd(t)}$ value is −3.6 to −0.7. The corrected $^{87}Sr/^{86}Sr$ ratios and ε_{Nd} values of the meta-sedimentary rocks are 0.707735 to 0.709379 and −3.6 to −0.4, respectively, whereas the values of the meta-volcanic rocks are 0.705597 to 0.709685, and −1.7 to 0.4 respectively. Note that the range of volcanic rocks marginally overlaps the range of sulfides (Fig. 9). Hence, it is reasonable to conclude that the sulfides were mainly derived from volcanic rocks, at the same time as the sediments were contributing to the hydrothermal system. Moreover, our results are consistent with those of previous studies of the regional igneous rocks: initial $^{87}Sr/^{86}Sr$ ratios and $\varepsilon_{Nd(t)}$ of granite and volcanics within the region range from 0.705 to 0.714 and 4.3 to −2.1, respectively (Zhao et al., 1993; Chen and Jahn, 2002). Therefore the rocks and ores were dominantly derived from juvenile material that had a strong crustal contamination. In fact, the conclusions from the Sr–Nd isotopes are consistent with those from trace element geochemistry. As mentioned above, the trace elements in the meta-volcanic rocks also show a strong crustal signature. For instance, the HFSEs Ta, Zr, and Hf are depleted relative to the LILEs Rb, Ba. The decoupled characteristics may be caused by fluid dehydration from the subduction slab. The low Ta/Yb ratio of the meta-volcanic rocks causes the data to plot in the VAG field (Fig. 8). We compare the Sr–Nd isotopic compositions of the deposits in IPB (see compilation in Tornos et al., 2005) with Keketale and find that both plot in a similar area, and therefore both show a mixed source (Fig. 9).

In Fig. 10a, b, Pb isotopes of the ores form a linear array, straddling the "orogen" curve. Most Pb-isotopic compositions of meta-sedimentary and meta-volcanic rocks show a narrow range near the "orogen" curve, except for a single meta-volcanic rock that is much more radiogenic than the others. The μ values for ores, meta-sedimentary and meta-volcanic rocks are similar. It is worth noting that Pb in the meta-sedimentary and meta-volcanic rocks should be of a mixed origin between mantle and crust comparable to the "orogen" reservoir of Zartman and Doe (1981). High $^{207}Pb/^{204}Pb$ values in the ores are evidence of crustal contamination. The conclusion inferred from the Pb isotopes is consistent with the data from the Sr–Nd isotopic system. Chiaradia et al. (2006) inferred a dominantly juvenile (mantle-derived) Pb contribution with some crustal contributions in the whole Chinese Altay orogen, and in the Keketale area the Pb isotopes of ores are also more radiogenic than in other areas, supporting our idea of crustal contamination.

5.2. Mechanism of ore formation

The ore-forming mechanism of the Keketale deposit is a matter of debate. Several authors proposed that it is transitional between SEDEX- and VMS-types of deposit, and refer to this type of deposit as "Altay" type (Wang et al., 1998, 1999). The ore is hosted in the Upper Sub-Kangbutiebao formation which has a total thickness of 1270 m. It is, however, restricted to a 160 m-thick interval of interlayered sandstone and rhyolite. The host sedimentary package represents a pause between two distinct volcanic events. As discussed above, the Sr–Nd–Pb isotope data suggest that the metal source was mainly the volcanic rocks (Figs. 9 and 10), and our S isotopes from disseminated and vein-type ores clearly show a magmatic signature. The ore-forming material for a VMS-type deposit is generally either leached from underlying volcanic rocks (e.g., Franklin et al., 1981; Lydon, 1988), or sourced directly from a magma (Herzig et al., 1998; Yang and Scott, 2002). Our new geochemical data can support either of the two mechanisms–or a mixture of the two–and provide strong evidence that the volcanic rocks contributed ore-forming material to the Keketale deposit. Keketale should be described as a VMS-type deposit, not an "Altay" type deposit.

A widely accepted ore genesis model for VMS deposits is that massive sulfides form at or near the seafloor through precipitation of sulfide from hydrothermal fluids that have interacted with underlying rocks. Specifically at the Keketale deposit, we propose that the early Devonian volcanic rocks were involved in the ore-forming processes (Fig. 12). Both the present and the previous studies of sulfur isotopes indicated a strong contribution of sulfur from seawater, therefore seawater must have been involved in the fluid circulation. We envisage that the seawater might become heated and evolve into an ore-forming hydrothermal fluid because of circulation through volcanic rocks during a hiatus in volcanic activity. The fluids then circulated through the rocks and leached metals. This was then transferred to the vents, allowing precipitation of sulfides on the seafloor. Simultaneously, marine sediments were deposited with the sulfides, so the direct host is sandstone. After the Keketale deposit formed, the volcanic activity was renewed and produced more volcanic rocks that both covered and preserved the sandstone and ores.

5.3. Tectonic setting of ore formation

VMS-type deposits always form in an extensional regime (Franklin et al., 1981; Sillitoe, 1982). Geological and lithological evidence suggest that the whole SAMB formed in an extensional regime. Firstly, the SAMB composed of a serious of volcanic sedimentary basins; Secondly, the volcanic rocks in those basins are dominated by rhyolitic rocks and minor basaltic rocks (Yu et al., 1993), so they represent a suite of bimodal volcanic rocks. The lithological assemble of bimodal volcanic rocks could be an indicator of extensional regime (Sonder and Jones, 1999; Foster and Gray, 2003). However, which mechanism caused such an extensional regime in the SAMB is still hotly debated. It has been suggested to either represent a rift on a passive continental margin (Chen et al., 1996; Wang et al., 1998, 1999) or a subduction-related setting (Windley et al., 2002; Xiao et al., 2004; Wan and Zhang, 2006). In Fig. 7b, we see a strong decoupling between HFSE and LILE of the underlying meta-rhyolitic lava; HFSE are depleted relative to LILE. Such a trend can be explained by fluid dehydration from a subduction slab, and we note that the patterns of our data are similar to those of the Chile island arc granite (Pearce et al., 1984). Pearce et al. (1984) proposed that Rb, Y (or Yb) and Nb (or Ta) are likely to be the most effective elements for the tectonic discrimination of felsic igneous rocks, and that a Ta *vs.* Yb plot represents the most likely projection in order to be alteration-independent. Therefore, we chose Ta *vs.* Yb to discriminate between different tectonic settings. All meta-rhyolitic rocks plot within the volcanic arc field (Fig. 8). The Sr–Nd–Pb isotope patterns of the Keketale ores and surrounding rocks show a clear

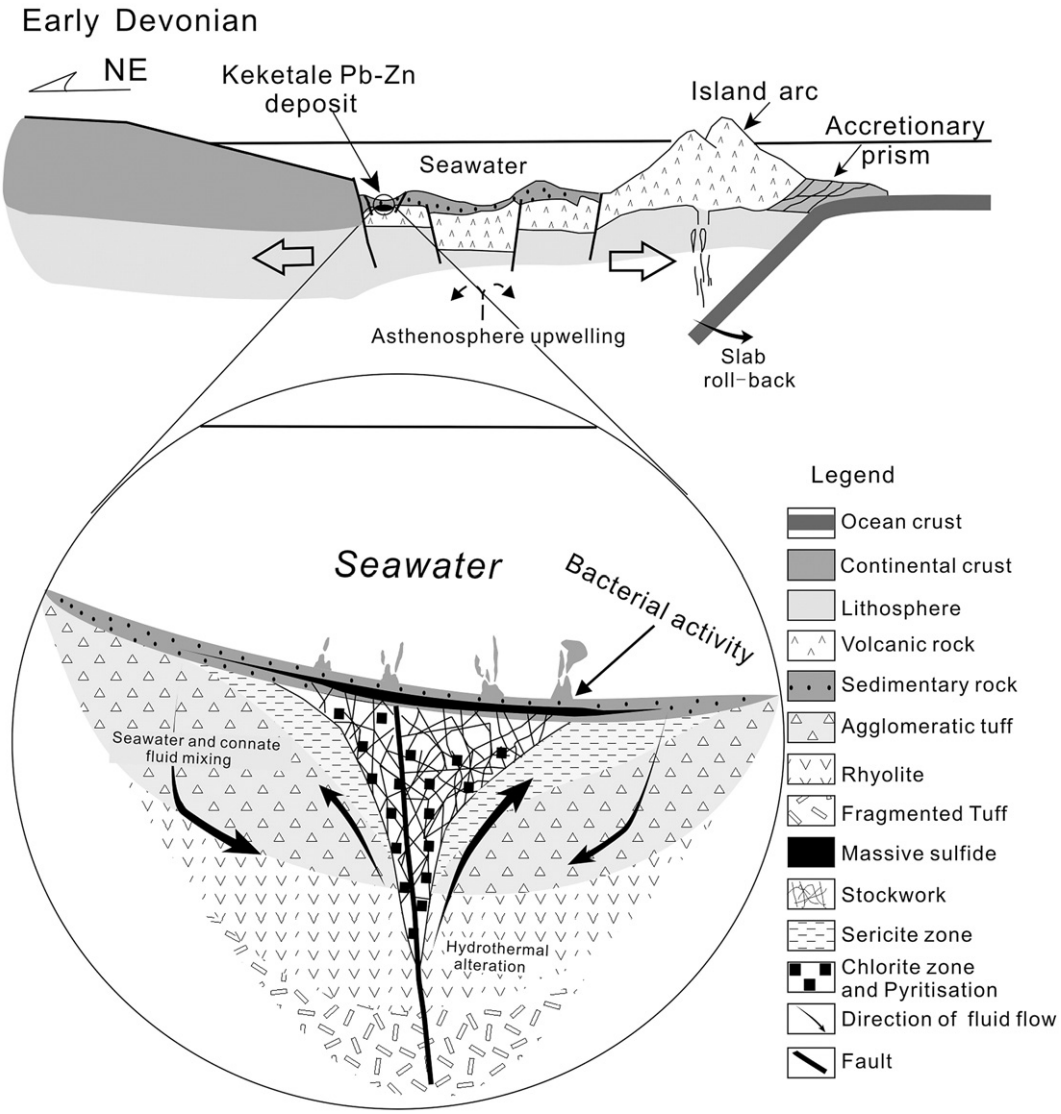

Fig. 12. Proposed genetic model for the Keketale Pb–Zn deposit. General sketch shows the tectonic setting of the Keketale ore deposit. Thermal and chemical zoning are indicated schematically in the enlarged drawing, which also shows the role of fractures in the focused hydrothermal circulation and during ore deposition. See text for additional explanation.

mixed source between mantle and crust (Figs. 9 and 10), and therefore, a subduction-related setting seems plausible. All geochemical and isotopic indicators in this study support formation of the Keketale deposit in a subduction-related setting. Windley et al. (2002) proposed that the Abagong unit formed in an intra-oceanic island arc setting, and (Xu et al., 2002) proposed that it formed in a back-arc basin. Here we further propose that the unit might contain both an island arc and a back-arc basin a situation similar to SW Pacific (Hall, 2002). Based on the regional geology, the Abagong unit consists of a series of volcanic sedimentary basins, and the Keketale formed in the Maizi basin — one of the four volcanic basins (Ashele, Chonhuer, Kelang and Maizi). Many other VMS deposits in the SAMB share similar characteristics with Keketale (e.g., Abagong, Tiemuerte, Akeharen, and Daqiao). The host strata of these deposits are the same as those at Keketale, and the Upper Kangbutiebao Formation hosts a stratabound Cu deposit (Wang et al., 1999; Jiang, 2003). The Mengku iron deposit is a metamorphosed, stratabound VMS deposit (Wang et al., 2003), which is hosted by the Lower Kangbutiebao Formation that has a SHRIMP U–Pb zircon age of 412 Ma (Chai et al., 2008). Therefore, we propose that Keketale and other VMS deposits formed in an arc or back-arc basin during the early Devonian; this would be consistent with an extensional regime. We prefer the back-arc basin model because of the extensive crustal-contaminated geochemical signatures, but we cannot exclude the possibility of an intra-arc basin setting. We further point out that the back-arc basin is a first-order basin, itself containing several smaller basins. Each of these volcanic basins (Chonhuer, Kelang and Maizi) is a second-order basin hosting many different types of deposits. The Keketale deposit formed in a third-order basin within one of the second-order basins; the other VMS deposits in the belt similarly are believed to have formed within comparable third-order basins.

In SAMB, the Ashele basin has commonly been considered to be an oceanic island arc produced when the Junggar plate subducted northwards (Niu et al., 2006; Sun et al., 2008). This interpretation is supported by the recent geochemical data of Ashele (Niu et al., 2006; Yuan et al., 2007; Wan et al., 2010). Niu et al. (2006) reported that boninite has been found in the area, and therefore they proposed a fore-arc setting. Boninite alone cannot be an indicator of a fore-arc setting, because it has also been identified in a back-arc setting (Piercey et al., 2001). Ashele can be considered to be an oceanward locality with respect to the Chonhuer, Kelang and Maizi basins. Firstly, the Ashele basin contains far more mafic volcanic rocks, and correspondingly less sedimentary rocks than the Chonhuer, Kelang and Maizi basins, and the rocks are isotopically more depleted (Fig. 9).

The Ashele deposit is mined for Cu and Zn, and its host stratum is a suite of early–middle Devonian (378 ± 39 Ma; Rb–Sr whole rock; Li and Chen, 2004) basaltic and dacitic rocks, which are different from the deposits mentioned above (Chen, 1990). In such a trench–arc–basin system, the mineralizing age of VMS deposits get younger towards the oceanward side, hence it is reasonable to propose that all VMS deposits in the SAMB formed during extensional process caused by slab roll-back. An early roll-back and consequent asthenosphere upwelling caused the opening of the back-arc basin, and Keketale and other similar VMS deposits, except Ashele, formed. During the late stage of this subduction slab roll-back, the island arc itself was in an extensional regime and the Ashele deposit formed. Our geochemical data suggest that mineralization of the Keketale deposit involved both crustal and mantle contributions. All other deposits share similar characteristics as the Keketale deposit, and these were important crustal contributions to the whole mineralization in the SAMB. Such a kind of metallogeny cannot be explained by a single arc system, as proposed by Sengör and Natal'in (1996). Therefore, a model of a Cordilleran-style orogen is more appropriate to the Chinese Altai in the Paleozoic.

6. Conclusions

The Keketale Pb–Zn deposit is a representative VMS deposit for the Southern Altai Metallogenic Belt; the whole ore district lies within a subduction-related basin regime. Based on our investigation of the geochemical characteristics of the deposits, we reach the following conclusions:

(1) The main orebodies of the Keketale deposit are bedded and laminated lenses stratabound within Lower Devonian volcanic sedimentary rocks; a stockwork of vein sulfide mineralization and chlorite- and sericite zone alteration occurs immediately around the ore lenses;
(2) Geochemical and isotopic data indicate that the ore-forming source had a mixed origin, and the ore-forming material originated from the underlying volcanic rocks and the host sedimentary rocks;
(3) All geochemical indicators support formation of the Keketale deposit in a subduction-related setting.

Combining our results with the regional and local geology, we propose that the Keketale deposit formed in a third-order basin within a back-arc basin. We further propose that all VMS deposits in the SAMB formed during slab roll-back.

Acknowledgments

This study is financially supported by the Chinese National Basic Research 973 Program (2007CB411307), the Knowledge Innovation Program of the Chinese Academy of Sciences (80922920), the Innovative Program of the Chinese Academy of Sciences (KZCX2-YW-Q04-08), and National Natural Science Foundation (40725009). Zhenlin Guo is thanked for providing help in the field. We are indebted to Kezhang Qin for critical discussions, and to Yongfei Zheng, Massimo Chiaradia, Hans Albert Gilg, and two anonymous reviewers for helpful comments. Finally, we thank Brain Windley and Nigel Cook for improvement of the manuscript.

References

Boynton, W.V., 1984. Geochemistry of the rare earth elements: meteorite studies. In: Henderson, P. (Ed.), Rare earth Element Geochemistry. Elsevier, Amsterdam, pp. 63–114.
Chai, F., Mao, J., Dong, L., Yang, F., Liu, F., Geng, X., Yang, Z., 2008. SHRIMP zircon U–Pb dating and its significance for the metarhyolites in the Kangbutiebao Formation from Abagong iron deposit at the southern margin of the Altay, Xinjiang. Acta Geological Sinica 82, 1592–1601.
Chen, Z.F., 1990. Ore-controlling factors and origin of the Ashele massive Cu–Zn sulphide deposit, Aletai, Xinjiang. Geology and Prospecting 7, 19–23 (in Chinese with English abstract).
Chen, L.H., Han, B.F., 2006. Geochronology, geochemistry and Sr–Nd–Pb isotopic composition of mafic intrusive rocks in Wuqiagou area, north Xinjiang: constraints for mantle sources and deep processes. Acta Petrologica Sinica 22 (5), 1201–1214 (in Chinese with English abstract).
Chen, B., Jahn, B.M., 2002. Geochemical and isotopic studies of the sedimentary and granitic rocks of the Altai orogen of northwest China and their tectonic implications. Geological Magazine 139 (1), 1–13.
Chen, Y.C., Ye, J.T., Fen, J., 1996. Ore-Forming Conditions and Metallogenic Prognosis of the Ashele Copper–Zinc Metallogenic Belt, Xinjiang, China. Geology Publishing House, Beijing. 330 pp.
Chen, H.L., Li, Z.L., Yang, S.F., Dong, C.W., Xiao, W.J., Tainosho, Y., 2006. Mineralogical and geochemical study of a newly discovered mafic granulite, northwest China: implications for tectonic evolution of the Altay Orogenic Belt. Island Arc 15 (1), 210–222.
Chen, F., Li, X., Wang, X., Li, Q., Siebe, W., 2007. Zircon age and Nd–Hf isotopic composition of the Yunnan Tethyan belt, southwestern China. International Journal of Earth Sciences 96 (6), 1179–1194.
Chiaradia, M., Konopelko, D., Seltmann, R., Cliff, R., 2006. Lead isotope variations across terrane boundaries of the Tien Shan and Chinese Altay. Mineralium Deposita 41 (5), 411–428.
Coleman, R.G., 1989. Continental growth of northwest China. Tectonics 8, 621–635.
Cong, F., Tang, H.F., Su, Y.P., 2007. Geochemistry and tectonic setting of Devonian rhyolites in southern Altay, Xinjiang, northwest China. Geotectonica et Metallogenia 31 (3), 359–364 (in Chinese with English abstract).
Foster, D.A., Gray, D.R., 2003. Evolution and structure of the Lachlan Fold Belt (Orogen) of Eastern Australia. Annual Review of Earth and Planetary Sciences 28 (1), 47–80.
Franklin, J.M., Lydon, J.W., Sangster, D.F., 1981. Volcanic-associated massive sulfide deposits. Economic Geology 75, 485–627 Anniversary Volume.
Goldfarb, R.J., Mao, J.W., Hart, C., Wang, D.H., Anderson, E., Wang, Z.L., 2003. Tectonic and metallogenic evolution of the Altay Shan, Northern Xinjiang Uygur Autonomous region, Northwestern China. In: Mao, J.W., Goldfarb, R.J., Seltmann, R., Wang, D.H., Xiao, W.J., Hart, C. (Eds.), Tectonic Evolution and Metallogeny of the Chinese Altay and Tianshan. Centre for Russian and Central Asian Mineral Studies, Natural History Museum, London, pp. 7–17.
Hall, R., 2002. Cenozoic geological and plate tectonic evolution of SE Asia and the SW Pacific: computer-based reconstructions, model and animations. Journal of Asian Earth Sciences 20 (4), 353–431.
He, G.Q., Han, B.F., Yue, Y.J., 1990. The tectonic evolution of Chinese Altai. Xinjiang Geology 2, 9–20 (in Chinese with English abstract).
Herzig, P.M., Hannington, M.D., Arribas Jr., A., 1998. Sulfur isotopic composition of hydrothermal precipitates from the Lau back-arc: implications for magmatic contributions to seafloor hydrothermal systems. Mineralium Deposita 33 (3), 226–237.
Huston, D., 1999. Stable isotopes and their significance for understanding the genesis of volcanic-associated massive sulfide deposits: A review. In: Hannington, M., Barrie, C. (Eds.), Volcanic-Associated Massive Sulfide Deposits: Processes and Examples in Modern and Ancient Settings. Society of Economic Geology, pp. 157–179.
Jiang, J., 2003. The mineral geology of the Tiemuert. Xinjiang Non-ferrous Metal 2, 2–5 (in Chinese).
Laurent-Charvet, S., Charvet, J., Shu, L.S., Ma, R.S., Lu, H.F., 2002. Palaeozoic late collisional strike–slip deformations in Tianshan and Altay, Eastern Xinjiang, NW China. Terra Nova 14 (4), 249–256.
Li, H.Q., Chen, F.W., 2004. Isotopic Geochronology of Regional Mineralization in Xinjiang, NW China. Geology Publishing House, Beijing. 391 pp.
Liu, W., 1990. Petrogenetic epochs and peculiarities of genetic types of granitoids in the Altai Mountains., Xinjiang Uygur Autonomous Region, China. Geotectonica Metallogenia 14, 43–56 (in Chinese with English abstract).
Long, X., Sun, M., Yuan, C., Xiao, W., Cai, K., 2008. Early Paleozoic sedimentary record of the Chinese Altai: implications for its tectonic evolution. Sedimentary Geology 208 (3–4), 88–100.
Lydon, J.W., 1988. Ore deposit models #14, volcanogenic massive sulphide deposits Part 2: genetic models. Geoscience Canada 15, 43–65.
Ma, G., Beaudoin, G., Qi, S., Li, Y., 2004. Geology and geochemistry of the Changba SEDEX Pb–Zn deposit, Qinling orogenic belt, China. Mineralium Deposita 39 (3), 380–395.
Niu, H., Sato, H., Zhang, H., Ito, J.I., Yu, X., Nagao, T., Terada, K., Zhang, Q., 2006. Juxtaposition of adakite, boninite, high-TiO2 and low-TiO2 basalts in the Devonian southern Altay, Xinjiang, NW China. Journal of Asian Earth Sciences 28 (4–6), 439–456.
Ohmoto, H., Rye, R.O., 1979. Isotopes of sulphur and carbon, In: Barnes, H.L. (Ed.), Geochemistry of Hydrothermal Ore Deposits, 2nd edition. John Wiley and Sons, New York, pp. 509–567.
Pearce, J.A., Harris, N.B.W., Tindle, A.G., 1984. Trace-element discrimination diagrams for the tectonic interpretation of granitic-rocks. Journal of Petrology 25 (4), 956–983.
Piercey, S.J., Murphy, D.C., Mortensen, J.K., Paradis, S., 2001. Boninitic magmatism in a continental margin setting, Yukon–Tanana terrane, southeastern Yukon, Canada. Geology 29 (8), 731–734.
Qin, K.Z., Wang, J.B., Zhang, J.H., Deng, J.N., 1998. The metallogenic condition of the Keketale type deposits in the southern margin of Altaid. Geological Exploration for Non-Ferrous Metals 2, 65–74 (in Chinese with English abstract).
Rui, Z.Y., Goldfarb, R., Qiu, Y.M., Zhou, T.H., Chen, R.Y., Pirajno, F., Yun, G., 2002. Paleozoic–early Mesozoic gold deposits of the Xinjiang Autonomous Region, northwestern China. Mineralium Deposita 37 (3), 393–418.
Sengör, A.M.C., Natal'in, B.A., 1996. Paleotectonics of Asia: fragments of a synthesis. In: Harrison, M., Yin, A. (Eds.), The Tectonic Evolution of Asia. Cambridge University Press, Cambridge, pp. 486–640.

Sengör, A.M.C., Natal'in, B.A., Burtman, V.S., 1993. Evolution of the Altaid tectonic collage and Palaeozoic crustal growth in Eurasia. Nature 364, 299–307.
Sillitoe, R.H., 1982. Extensional habitats of rhyolite-hosted massive sulfide deposits. Geology 10, 403–407.
Sonder, L.J., Jones, C.H., 1999. Western United States extension: how the West was widened. Annual Review of Earth and Planetary Sciences 27 (1), 417–462.
Sun, M., Yuan, C., Xiao, W., Long, X., Xia, X., Zhao, G., Lin, S., Wu, F., Kroner, A., 2008. Zircon U–Pb and Hf isotopic study of gneissic rocks from the Chinese Altai: progressive accretionary history in the early to middle Palaeozoic. Chemical Geology 247 (3–4), 352–383.
Tornos, F., 2006. Environment of formation and styles of volcanogenic massive sulfides: the Iberian Pyrite Belt. Ore Geology Reviews 28 (3), 259–307.
Tornos, F., Casquet, C., Relvas, J.M.R.S., 2005. 4: Transpressional tectonics, lower crust decoupling and intrusion of deep mafic sills: a model for the unusual metallogenesis of SW Iberia. Ore Geology Reviews 27 (1–4), 133–163.
Tornos, F., Solomon, M., Conde, C., Spiro, B.F., 2008. Formation of the Tharsis Massive Sulfide Deposit, Iberian Pyrite Belt: geological, lithogeochemical, and stable isotope evidence for deposition in a brine pool. Economic Geology 103 (1), 185–214.
Velasco, F., Sanchez España, J., Boyce, A., Fallick, A.E., Sáez, R., Almodóvar, G.R., 1998. A new sulphur isotopic study of some Iberian Pyrite Belt deposits: evidence of a textural control on some sulphur isotope compositions. Mineralium Deposita 34, 1–18.
Wan, B., Zhang, L.C., 2006. Sr–Nd–Pb isotope geochemistry and tectonic setting of Devonian polymetallic metallogenic belt on the Southern margin of Altaid, Xingjing. Acta Petrologica Sinica 22 (1), 145–152 (in Chinese with English abstract).
Wan, B., Zhang, L.C., Xiang, P., 2010. The Ashele VMS-type Cu–Zn deposit in Xinjiang, NW China formed in a rifted arc setting. Resource Geology 60 (2).
Wang, J.B., Qin, K.Z., Wu, Z.L., Hu, J.H., Deng, J.N., 1998. Volcanic-Exhalative-Sedimentary Lead–Zinc Deposits in the Southern Margin of the Altai, Xinjiang. Geology Publishing House, Beijing. 210 pp.
Wang, J.B., Deng, J.N., Zhang, J.H., Qin, K.Z., 1999. Massive sulphide deposits related to the volcano-passive continental margin in the Altay region. Acta Geological Sinica 73, 253–263.
Wang, Y.W., Wang, J.B., Wang, S.L., Ding, R.F., Wang, L.J., 2003. Geology of the Mengku iron deposit, Xinjing, China: a metamorphosed VMS? In: Mao, J.W., Goldfarb, R.J., Seltmann, R., Wang, D.H., Xiao, W.J., Hart, C. (Eds.), Tectonic Evolution and Metallogeny of the Chinese Altay and Tianshan. Centre for Russian and Central Asian Mineral Studies, Natural History Museum, London, pp. 181–200.
Wang, T., Hong, D.W., Jahn, B.M., Tong, Y., Wang, Y.B., Han, B.F., Wang, X.X., 2006. Timing, petrogenesis, and setting of Paleozoic synorogenic intrusions from the Altai Mountains, Northwest China: implications for the tectonic evolution of an accretionary orogen. Journal of Geology 114 (6), 735–751.
Wei, C., Clarke, G., Tian, W., Qiu, L., 2007. Transition of metamorphic series from the Kyanite- to Andalusite-types in the Altai orogen, Xinjiang, China: evidence from petrography and calculated KMnFMASH and KFMASH phase relations. Lithos 96 (3–4), 353–374.
Windley, B.F., Kröner, A., Guo, J.H., Qu, G.S., Li, Y.Y., Zhang, C., 2002. Neoproterozoic to Paleozoic geology of the Altai Orogen, NW China: new zircon age data and tectonic evolution. Journal of Geology 110, 719–737.
Windley, B.F., Alexeiev, D., Xiao, W.J., Kröner, A., Badarch, G., 2007. Tectonic models for accretion of the Central Asian Orogenic Belt. Journal of the Geological Society of London 164, 31–47.
Xiao, W.J., Windley, B.F., Badarch, G., Sun, S., Li, J.L., Qin, K.Z., Wang, Z.H., 2004. Palaeozoic accretionary and convergent tectonics of the southern Altaids: implications for the growth of Central Asia. Journal of Geology Society London 161, 339–342.
Xu, J.F., Castillo, P.R., Chen, F.R., Niu, H.C., Yu, X.U., Zhen, Z.P., 2002. Geochemistry of late Paleozoic mafic igneous rocks from the Kuerti area, Xinjiang, northwest China: implications for backarc mantle evolution. Chemical Geology 193 (1–2), 137–154.
Yang, K., Scott, S.D., 2002. Magmatic degassing of volatiles and ore metals into a hydrothermal system on the modern sea floor of the eastern Manus back-arc basin, western Pacific. Economic Geology 97, 1079–1100.
Ye, Q.T., Fu, X.J., Zhang, X.H., 1997. Geological characteristics and genesis of the Ashele copper–zinc massive sulphide deposit, Xinjiang. Mineral Deposits 16, 96–106 (in Chinese with English abstract).
Yu, X.Y., Mei, H.J., Yang, X.C., 1993. The volcanic and tectonic evolution of Erqis. In: Tu, G.Z. (Ed.), Progress of Solid Earth Sciences in Northern Xinjiang, China. Science Press, Beijing, pp. 185–199.
Yuan, C., Sun, M., Xiao, W., Li, X., Chen, H., Lin, S., Xia, X., Long, X., 2007. Accretionary orogenesis of the Chinese Altai: insights from Paleozoic granitoids. Chemical Geology 242 (1–2), 22–39.
Zartman, R.E., Doe, B.R., 1981. Plumbotectonics—the model. Tectonophysics 75, 135–162.
Zhang, J.H., Wang, J.B., Ding, R.F., 2000. Characteristics and U–Pb ages of Zircon in metavolcanics from the Kangbutiebao formation in the Altai Orogen, Xingjiang. Regional Geology of China 19, 281–287 (in Chinese with English abstract).
Zhang, Z., Mao, J., Chai, F., Yan, S., Chen, B., Pirajno, F., 2009. Geochemistry of the Permian Kalatongke Mafic Intrusions, Northern Xinjiang, Northwest China: implications for the genesis of magmatic Ni–Cu sulfide deposits. Economic Geology 104 (2), 185–203.
Zhao, Z.H., Wang, Z.G., Zou, T.R., Masuda, A., 1993. The REE, isotopic composition of O, Pb, Sr and Nd and petrogenesis of granitoids in the Altai region. In: Tu, G.Z. (Ed.), Progress of Solid Earth Sciences in Northern Xinjiang, China. Science Press, Beijing, pp. 239–266.
Zhuang, Y.X., 1994. Tectonothermal Evolution in Space and Time and Orogenic Process of Altaide, China. Jilin Scientific and Technical Press, Changchun, China. 402 pp.
Zindler, A., Hart, S., 1986. Chemical geodynamics. Annual Reviews of Earth and Planetary Sciences 14, 493–571.
Zou, T., Cao, H., Wu, B., 1988. Orogenic and anorogenic granitoids of the Altay mountains, Xinjiang and their discrimination criteria. Acta Geological Sinica 3, 228–245 (in Chinese with English abstract).